1986ApJ...308..815N

THE ASTROPHYSICAL JOURNAL, 308:815–828, 1986 September 15
© 1986. The American Astronomical Society. All rights reserved. Printed in U.S.A.

QUASARS MEASURED BY THE *INFRARED ASTRONOMICAL SATELLITE*

G. NEUGEBAUER
Palomar Observatory, California Institute of Technology
G. K. MILEY
Space Telescope Science Institute[1] and Sterrewacht, Leiden, The Netherlands
B. T. SOIFER
Palomar Observatory, California Institute of Technology
AND
P. E. CLEGG
Queen Mary College, London
Received 1986 January 16; accepted 1986 February 27

ABSTRACT

Measurements from 12 to 100 μm of 179 quasars observed with the *IRAS* satellite are presented; of these 74 have detections with signal-to-noise ratios greater than four in at least one wavelength band. The infrared flux densities of the quasars with flat radio spectra generally lie on a smooth interpolation between measurements at visible and radio wavelengths. For the radio quiet quasars the peak in the flux densities appears in the far-infrared. The luminosities near 60 μm of the flat spectrum radio sources extend to significantly higher values than do those of the radio quiet quasars or those with steep radio spectral indexes. The infrared luminosities range up to $10^{13.9}\ L_{\odot}$. From these observations there are no infrared properties of quasars that are strongly correlated with their radio properties.

There is strong circumstantial evidence from the observations that the infrared emission from the quasars whose radio emission has a flat spectrum is predominantly nonthermal in origin. For the radio quiet quasars and those with steep radio spectra, there is evidence that the emission is at least partially thermal.

Subject headings: infrared: sources — quasars

I. INTRODUCTION

Although active galaxies are often conspicuous emitters of infrared radiation, the role of the infrared in the energetics of quasars, and the origin of the infrared continuum emission, is poorly understood. Several observational studies of quasars in the near-infrared have been published [see, e.g., Neugebauer *et al.* (1979), Glass (1979) and Cutri *et al.* (1985)], but only occasional measurements in the far-infrared and submillimeter wavelengths of well-known and bright quasars have been possible because of limited sensitivity at these wavelengths [see, e.g., Harvey, Wilking, and Joy (1982); Clegg *et al.* (1983)].

The all-sky survey of the *Infrared Astronomical Satellite* (*IRAS*) plus the pointed observations that were part of that mission have provided measurements in the far-infrared for a large number of quasars. In this paper we describe the *IRAS* observations of 179 quasars and compare the infrared properties of these quasars with their properties at other wavelengths. The continuum energy distributions of several representative quasars over a wide frequency range have been presented by Neugebauer, Soifer, and Miley (1985), by Bregman *et al.* (1986) and by Landau *et al.* (1986) and will not be repeated here. Rather, we will concentrate on presenting the statistical properties of the sample. In particular we will search for general trends, such as peaks in the energy distributions or evidence for emission from the host galaxies, which might provide clues as to the mechanism producing the infrared continuum.

[1] On contract from European Space Agency.

II. OBSERVATIONS

The *IRAS* survey has been described in general by Neugebauer *et al.* (1984*a*) and in detail in the *IRAS Explanatory Supplement* (1985). The sensitivity limits ($\sim$0.5 Jy at 12, 25, and 60 μm and 1.5 Jy at 100 μm) of the all-sky survey for point sources are such that only 21 quasars were detected in the *IRAS Point Source Catalog* (1985) where quasars will be arbitrarily restricted to be those objects defined to be quasars in the catalog by Veron-Cetty and Veron (1985; henceforth VCV). This definition includes "a starlike object, or object with a starlike nucleus, brighter than absolute (visual) magnitude -23 [$H_0 = 50$ km s^{-1} Mpc^{-1}; $q_0 = 0$].

The most sensitive observations of quasars with *IRAS* were obtained by means of "pointed observations" of preselected objects carried out in addition to the *IRAS* all-sky survey. These observations were made by repeatedly scanning the telescope field of view over preselected targets (Young *et al.* 1985). Typically about 8 min of actual observing time was accorded to a single pointed observation sequence, resulting in an increase in sensitivity above the survey for a point source by a factor of about 5. For some targets, as many as 10 pointed observing sequences were carried out, and a minimum of two separate sequences was required in order to discriminate against noncelestial objects such as asteroids or radiation hits. The data were processed to yield maps of the $0\overset{\circ}{.}5 \times 1\overset{\circ}{.}5$ area around the target giving both the total infrared intensity and the results of a spatial filtering applied to increase the sensitivity for pointlike sources.

In several observations, especially at 100 μm and to some extent at 60 μm, "Galactic infrared cirrus" (Low *et al.* 1984) was obviously present and determined the detection threshold

© American Astronomical Society • Provided by the NASA Astrophysics Data System

1986ApJ...308..815N

of the observations. In others, the detections of the quasar was obviously limited by neighboring infrared sources. This occurred most often in the 60 or 100 μm wavelength bands where the detectors were larger than at 12 and 25 μm. Often the effects of cirrus and confusing sources were indistinguishable. Only two sources observed with the pointed observations were so clearly confused by nearby infrared sources as to be unmeasurable in all four bands, and these were omitted from the sample. Some 45 sources were contaminated in at least one band by nearby infrared sources or cirrus.

An infrared source was identified with the quasar if it was within 1′ of the optical or radio position and was in a relatively clear field. The differences between the location of the 60 μm source and the nominal positions (taken from VCV) in a direction parallel to the *IRAS* telescope scan motion form a distribution with full width at half-maximum of 20″; 90% of the infrared sources were observed to be within $\pm 20''$ of the nominal position. In the direction perpendicular to the scan direction, 90% of the infrared sources lie within $\pm 40''$ of the nominal position. Both of these distributions are completely consistent with the pointing accuracy of the pointed observations as described by Young *et al.* (1985).

Although the *IRAS* mission lasted some 9 months, the geometry of the scanning patterns and the high priority assigned to the all-sky survey meant that few pointed observations were repeated with a sufficient time interval between them to search for variability. One exception is the quasar 1641+399 (3C 345) which was observed with pointed observations near the beginning and end of the mission. Significant variability of this object was observed over a 7 month period and is described by Bregman *et al.* (1986). The quasar 2223−052 (3C 446) was observed in pointed observations only at the end of the mission, but was bright enough to be cataloged in the *Point Source Catalog* early in the mission. The observations of 3C 446, which was also seen to vary strongly, are discussed below; a further study of the variability of quasars as observed by *IRAS* is in progress.

III. SAMPLE

A variety of quasars was included in the list of target objects for pointed observations. This included samples of high and low redshift quasars, samples of radio loud and radio quiet quasars, samples of quasars whose radio emission was dominated by emission from either extended lobes or compact cores and samples of visually bright quasars. Often an attempt was made to schedule multiple sequences of pointed observations for objects which were predicted to be faint in the *IRAS* wavelength bands.

The pointed observations were accorded lower priority in the scheduling of the telescope observing time than the all-sky survey. In addition, there were several natural constraints which degraded the observations with the satellite in certain locations or restricted the field of view of the telescope. As a result, the targeted objects were not observed purely in the order of their scientifically assigned priority. Often quasars with high scientific interest were not observed, while objects with low interest, but in a more accessible area of the sky, were observed repeatedly.

The results of the pointed observations made of quasars are included in Table 1. The noise level of the observations was derived from the median noise over the 0°.5 × 1°.5 map; these noise estimators are described by Young *et al.* (1985). Limits are given as 3 times the median noise levels of the maps; detections at a signal-to-noise ratio below three were, however, sometimes possible depending on the noise characteristics in the neighborhood of the target. The presence of a bright source, including bright infrared cirrus, close to the location of the quasar could also hide signals in the wings of the spatial filter. Thus the limits, especially where confusion or cirrus is indicated, should be viewed with some skepticism. A subjective indication, based largely on the presence of extended sources seen only at 100 μm, that Galactic cirrus was present is also included in Table 1. Since limits associated with confusing sources or the presence of cirrus are so uncertain and subjective, sources so identified in Table 1 have been omitted from the statistical studies given below. In the statistical analysis, detections with signal-to-noise ratios less than four have also been treated as limits at 4 times the noise level.

It is estimated from surface density counts that 1.6% of the quasars observed would be contaminated by a galaxy at the level of 60 mJy. In addition, the quasars detected by *IRAS* were examined on the plates of the Palomar Schmidt or ESO surveys to eliminate accidental contamination by nearby galaxies; of about 80 examined, one quasar was contaminated by a nearby galaxy.

Six quasars which were not observed in the program of pointed observations were detected in at least one wavelength band in the survey and cataloged in the *IRAS Point Source Catalog* (1985). The flux densities of these quasars are also included in Table 1. Although the quasars were selected on the basis of their inclusion in the *IRAS Point Source Catalog*, the flux densities in Table 1 were obtained from subsequent reprocessing of the observations which enhanced the sensitivity of the survey measurements. Finally, there are 13 quasars with visual magnitudes brighter than 15 mag listed in VCV but not included in the pointed observations or cataloged in the *IRAS Point Source Catalog*. The survey observations in the areas around these quasars were subsequently reprocessed and the results included in Table 1; six of the 13 quasars so selected were detected in at least one *IRAS* wavelength band.

In total, measurements of 179 quasars are given in Table 1. Seventy-four of these have detections with signal-to-noise ratios exceeding four in one or more of the *IRAS* wavelength bands. Of these 74, only nine have redshifts greater than 1.00 and only two have redshifts in excess of 2.00. The quasar 2126−158 was detected at 60 μm with a signal-to-noise ratio of four; its redshift of 3.275 was the largest associated with a quasar detected by *IRAS*.

IV. DISCUSSION OF STATISTICAL PROPERTIES

a) Luminosity

Luminosities were approximated by calculating the luminosity per logarithmic frequency interval, νL_ν, at the rest wavelengths of 12, 25, 60, and 100 μm; L_ν is the luminosity per unit frequency interval at the frequency ν. Isotropic emission has been assumed. Thus it should be cautioned that current theories of beamed emission may predict significantly different luminosities, especially if the quasar is variable. A Hubble constant of $H_0 = 75$ km s^{-1} Mpc^{-1} and deceleration parameter of $q_0 = 0.5$ was used; these values will be adopted throughout this paper. In order to correct to the rest frequencies, intrinsic spectral indexes α were assumed to be those obtained from the measurements when available, or -1 when measurements in neighboring wavelength bands were unavailable. The spectral index is defined throughout this paper so that the flux density $f_\nu \sim \nu^\alpha$. The luminosities in the visible, taken to be at 0.55 μm

© American Astronomical Society • Provided by the NASA Astrophysics Data System

1986ApJ...308..815N

TABLE 1

FLUX DENSITIES

Object	12 μm mJy	25 μm mJy	60 μm mJy	100 μm mJy	log(L(60)/L⊙)	remarks[1]
0003+158	<36	<86	<67	<187	<11.60	S
0007+106	99±6	163±12	213±8	<845	10.64	F, 2
0017+257	<40	73±21	119±20	<155	11.42	I
0017+154	<59	<95	<84	<260	<13.13	S
0026+129	<18	<40	<27	<80	<10.15	Q
0029−414	33±13	<54	<66	<189	<12.24	F
0030+034	<38	<86	<67	<187	<13.02	Q
0033+183	<55	<109	<72	<204	<12.75	S
0046+112	<36	<86	<67	<187	<11.14	Q
0047−832	<42	<49	72±28	<324	12.48	I
0050+124	549±11	1097±20	2293±17	2959±51	11.33	Q
0051+291	<40	<63	<58	<175	<12.87	I, 3
0052+251	<80	<180	93±18	<338	10.77	Q
0054+144	72±7	86±13	291±9	794±26	11.39	Q
0054−226	<108	<127	<154	<347	<10.17	Q
0100+130	<18	<40	<27	<80	<12.91	Q
0109+176	<42	<73	<63	<194	<13.07	S
0110+297	<39	<59	<61	<180	<11.36	I, 3
0119−286	<110	<113	<154	<347	<10.71	Q
0119+247	<41	<60	<61	<178	<13.00	F
0121−590	397±9	598±10	623±15	756±44	10.48	Q
0127+233	<55	<105	<85	<244	<12.82	S
0130+242	<38	<79	<67	<187	<11.61	S
0131+055	<48	<78	<64	<161	<12.92	Q
0132+205	<38	<79	<67	<187	<12.91	Q
0134+329	56±6	160±8	770±9	1080±27	12.52	S
0157+001	137±38	520±58	2377±56	2322±130	12.23	Q
0202+319	<20	<32	<30	<87	<12.37	F
0202−172	<41	<61	82±21	<200	12.98	F, 3
0205+024	<60	130±21	82±16	<130	10.71	Q, 4
0229+131	<20	<45	<26	<79	<12.65	I
0234+285	<35	<65	187±18	<178	12.98	F, 2
0242−724	93±11	107±11	308±20	330±69	10.91	Q
0312−770	<37	<38	<62	<194	<10.92	F
0333+321	<36	<64	<97	<874	<12.74	F
0349−146	<32	<47	<49	<282	<11.76	S
0355−483	<41	<44	<78	<273	<12.44	I
0400+258	<40	<79	<57	<277	<13.01	F, 5
0405−123	<87	116±31	<126	<312	<12.10	F, 5
0410+110	68±16	178±29	261±24	<564	11.83	S
0420−014	25±10	92±17	271±16	565±61	12.96	I
0422−380	<31	<36	<50	<158	<12.00	F
0438−436	25±8	<28	120±14	279±47	13.62	F
0439−433	<25	<29	72±14	<282	11.88	S, 3
0506−612	<26	<29	<48	155±52	<12.29	F
0530−379	18±9	42±10	<48	<163	<11.05	Q
0537−441	149±10	298±11	631±25	808±91	13.14	F
0551−366	<27	<29	<49	<161	<13.03	Q
0607−157	<25	<34	54±13	<147	11.20	F, 3
0610+260	<41	<79	<67	<54	<11.83	S
0642+449	<34	<51	<51	<155	<13.42	S, 2
0704+384	<22	40±13	62±11	<101	11.13	S
0710+118	<41	<83	<57	<161	<12.03	S, 2
0710+457	233±27	551±33	864±44	439±107	10.83	Q
0711+356	<19	33±11	28±9	<87	12.44	F
0730+257	<50	<107	<71	<192	<13.33	S
0736+017	34±6	77±9	133±8	<564	11.11	F, 3
0738+313	<20	<39	145±9	<282	12.25	F, 3
0742+318	33±6	65±11	112±8	<141	11.84	I, 3
0742+333	<18	<32	<24	<141	<11.44	F, 3
0743−673	<39	<41	<66	<245	<12.74	S
0748+126	<37	<67	205±17	365±51	12.73	F
0751+298	<29	<74	<57	<155	<13.00	I
0752+258	<40	<93	<58	<172	<11.53	F
0754+394	94±31	336±42	<140	<347	<10.52	Q
0758+120	<51	<90	<76	<204	<13.36	S
0758+143	<52	<100	<79	<201	<12.60	S
0802+103	<50	<88	<77	<212	<13.06	S
0824+110	<39	<67	63±19	<161	13.13	F
0831+101	<52	<92	<77	<220	<12.96	F, 3
0836+195	<57	<124	59±20	<158	12.80	S
0837−120	32±11	49±16	69±15	94±45	10.83	S
0838+770	34±5	103±7	174±9	426±30	10.89	Q,6
0844+349	126±29	204±40	163±41	294±97	10.21	Q
0847+190	<40	<89	<54	<149	<11.72	Q
0906+484	39±6	87±8	172±10	291±32	10.79	Q,7
0923+392	<15	<26	<27	<80	<11.61	F
0953+414	<89	<107	<129	<315	<11.30	Q
0957+561	<33	<44	96±19	<282	12.82	S, 3
0958+551	<42	<65	<73	<212	<12.93	Q
1001+054	31±6	36±12	27±9	<69	10.26	Q
1059+730	18±6	51±7	<50	<169	<10.01	Q, 5
1100+772	17±5	45±6	61±9	<85	11.22	S, 3
1101−325	<39	<52	<67	<225	<11.38	F
1104+167	<20	<41	<25	<73	<11.49	I
1116−462	<41	<48	<86	<335	<12.14	I
1126−041	104±19	309±35	669±26	1172±134	10.78	Q, 2
1137+660	<39	<51	<64	<198	<11.93	S
1138+222	<110	<140	396±53	525±126	10.60	Q
1143−245	<55	<78	<79	<247	<13.07	F
1148−001	<45	<86	<64	<200	<12.99	F
1150+497	21±6	25±7	42±11	<108	11.12	I
1156+295	<20	33±11	<126	<85	<12.33	I,8
1206−399	<39	<55	<64	404±68	<12.30	F
1211+143	172±38	362±51	305±53	689±119	10.73	Q
1216−015	<118	<179	210±54	462±110	10.76	Q
1225+317	<38	<56	<58	<189	<13.06	F
1226+023	417±12	941±27	1805±14	3109±45	12.07	F
1227+024	<37	<82	<42	<135	<11.49	Q
1254+571	1856±9	9184±11	35257±16	34229±47	12.17	Q
1304+346	<38	<51	<62	<187	<10.75	Q
1308+182	<42	<61	<57	<178	<12.79	F
1351+640	173±5	532±6	757±8	1184±26	11.16	Q
1353+186	482±35	1380±37	2218±48	1986±125	11.14	Q
1358+043	<41	44±22	72±19	<169	11.58	Q
1404+286	<872	423±11	762±13	1052±39	11.05	F, 4
1411+442	115±10	160±12	162±17	<175	10.52	Q
1426+015	124±33	171±46	318±47	<315	10.78	Q
1435+638	<16	<18	<26	<79	<12.64	F, 3
1440+356	98±13	208±15	652±21	1061±64	11.02	Q
1442+101	<25	<37	<76	<169	<13.63	S, 5
1448+634	<84	<73	260±40	558±97	10.06	S
1449+588	43±9	60±11	123±16	342±52	11.19	Q
1502+106	<20	<30	<29	<85	<11.44	F
1511+103	<33	<48	<47	<149	<12.62	I
1512+370	<38	<42	61±20	<178	11.38	I
1517+239	<23	<33	<40	<134	<12.75	Q
1525+227	20±5	34±6	91±7	<132	11.20	I, 2
1538+477	<37	<41	<126	<282	<12.38	Q
1543+489	58±15	126±18	348±26	485±79	12.20	Q
1544+212	<31	<37	<47	<141	<12.87	Q
1545+209	<31	<37	<47	<141	<12.77	Q
1545+210	<31	<37	<50	<141	<10.98	I, 5
1545+210	<31	<37	<50	<141	<12.85	Q, 5
1548+114	<31	<43	66±16	<986	11.56	F, 3
1553+113	<86	<93	<123	<284	<11.66	Q
1606+289	<15	<18	<25	<76	<12.59	S
1611+343	24±4	12±4	<53	<141	<12.58	F, 5
1612+266	<33	<40	<54	<161	<11.38	Q
1612+261	<33	<40	<54	<161	<10.38	Q, 2
1613+658	87±12	231±14	635±19	1090±59	11.45	Q
1626+554	<38	<39	<70	<238	<10.51	Q
1631+627	<33	<40	<67	<214	<13.00	Q
1633+382	<15	11±5	36±8	<74	12.65	F
1634+628	<36	<37	<59	<186	<12.29	S
1634+706	61±13	147±14	318±23	343±72	13.16	Q
1634+267	<31	<38	<50	<168	<12.88	Q
1635+266	<31	<38	<50	<168	<12.87	Q
1637+574	<38	<39	<68	<206	<12.09	F
1640+396	<46	<48	<77	<240	<11.93	Q
1640+401	<46	<48	<77	<240	<12.41	Q
1641+399	144±10	338±11	766±18	1277±56	12.91	F,9
1700+518	120±23	220±21	480±36	482±88	12.01	Q
1702+298	<29	<34	<48	<155	<12.84	S
1704+608	46±5	125±5	183±9	< 299	11.86	S, 3
1726+499	<17	<19	<29	<704	<11.79	Q, 5
1807+279	<26	<33	<44	<141	<12.72	F
1821+643	236±19	373±18	953±32	2164±82	12.40	Q
1828+487	<21	<27	<38	<152	<11.75	S
1830+285	<38	44±15	<101	<564	<12.04	I, 5
1847+335	<27	<33	<43	<149	<11.52	Q
1912−550	<35	<41	<67	<282	<11.48	S,10
1916−587	268±24	351±26	672±35	914±122	10.36	Q
2000−330	<19	<35	<29	<85	<13.28	F
2041−109	350±31	667±44	1508±44	1607±104	10.66	Q
2059+034	<23	49±11	174±12	<114	13.13	F
2112+059	71±13	73±25	105±19	<177	11.83	Q
2120+168	<39	<62	<63	<214	<12.90	S
2126−158	<44	<81	84±20	<192	13.60	F
2128−123	<44	<96	<59	<185	<11.64	F, 3
2130+099	188±8	378±14	480±13	<1888	10.65	Q, 3
2141+175	<28	42±14	102±14	<423	11.09	F, 3
2142−758	<33	<37	<61	<220	<12.43	F
2201+315	62±6	111±7	126±9	<85	11.49	F
2204−573	<33	<40	<76	<282	<13.38	F, 5
2209+152	<40	<66	<64	<178	<12.73	I
2214+139	61±7	95±12	337±11	<282	10.58	Q, 3
2223−052	168±11	363±19	951±16	1747±51	13.88	F
2223+210	<38	<55	<59	<163	<12.95	F
2251+158	<41	112±18	179±19	<564	12.63	F, 2
2251+113	<36	<66	<67	<214	<11.29	I
2251+244	<17	<27	<92	<169	<13.31	I,11
2254+074	<41	<73	155±20	<366	12.05	I, 3
2300−683	<28	<32	<52	<172	<11.61	F
2314+038	<107	206±52	672±52	851±118	11.95	S
2326−477	<43	<56	<60	<132	<12.56	F,8
2344+092	<19	71±13	67±8	<135	11.98	F, 2
2345−167	37±15	<94	93±19	<158	11.97	F
2353−685	<38	<46	<64	<194	<12.86	F

NOTES.—(1) Q = radio quiet; F = flat radio spectrum; S = steep radio spectrum; I = intermediate radio spectrum; (2) 100 μm cirrus; (3) 100 μm confused; (4) 12 μm confused; (5) 60 and 100 μm confused; (6) 100 μm position off; flux density questionable; (7) 12 μm position off; flux density questionable; (8) 60 μm confused; (9) from Bregman *et al.* 1986; (10) 12 and 100 μm confused; (11) 60 and 100 μm cirrus.

© American Astronomical Society • Provided by the NASA Astrophysics Data System

1986ApJ...308..815N

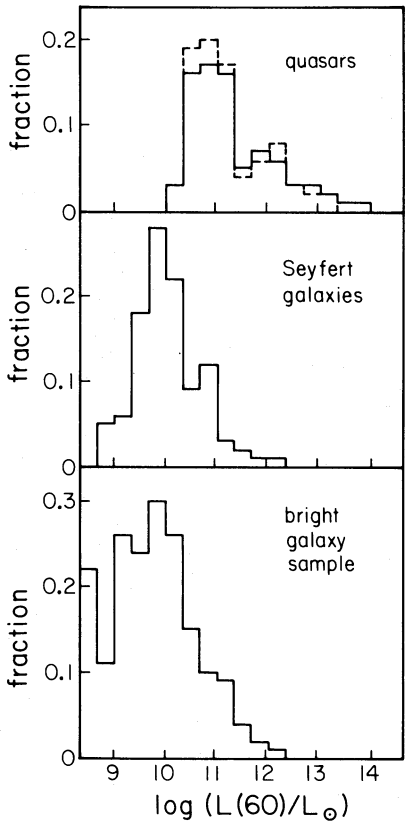

FIG. 1.—The fractional luminosity distribution at 60 μm for the present sample of quasars is given (*top*) for the entire sample (*solid line*) and for those quasars with $V < 17.1$ mag (*dashed line*). The luminosity distributions for Markarian and NGC galaxies classified as Seyfert 1 or 2 in VCV and found in the *IRAS Point Source Catalog* by Miley, Neugebauer, and Soifer (1985) (*middle*) and for a sample of *IRAS* galaxies brighter than 5 Jy at 60 μm selected by Soifer *et al.* (1986) (*bottom*) are also presented. The fractional luminosity distribution was obtained by dividing the number of sources of observed luminosity L in each luminosity bin by the number of sources in the sample, including those for which only limiting flux densities were obtained, that could have been observed if they had the luminosity L assigned to that bin.

in the rest frame, were calculated assuming a spectral index of -0.7 and the visual magnitudes given by VCV.

The fractional luminosity distribution at 60 μm for the sample of quasars is illustrated in Figure 1. The luminosity distributions for Markarian and NGC galaxies classified as Seyfert 1 or 2 in VCV and found in the *IRAS Point Source Catalog* by Miley, Neugebauer and Soifer (1985) and for a sample of *IRAS* galaxies brighter than 5 Jy at 60 μm selected by Soifer *et al.* (1986) are also given. The fractional luminosity distribution was obtained by dividing the number of sources of observed luminosity L in each luminosity bin by the number of sources in the sample, including those for which only limiting flux densities were obtained, that could have been observed if they had the luminosity L assigned to that bin (Elvis *et al.* 1978; Meurs and Wilson 1984).

The fractional luminosity distributions of (*a*) the quasars with a visual magnitude, as listed in VCV, of $V < 17.1$ mag [f_ν(vis) = 0.5 mJy] and of (*b*) all 179 quasars are both included in Figure 1. Miley, Neugebauer and Soifer (1985) have shown that the luminosity distribution for Seyfert galaxies is not dependent on whether the Seyfert galaxy is of Type 1 or 2 and thus these two types of Seyfert galaxies are combined in Figure 1. Although the samples represent significantly different selection criteria, the differences between the distributions are clear: quasars are typically a factor of 10 more luminous near 60 μm than are either the bright galaxies or the Seyfert galaxies and the distribution extends nearly two orders of magnitude above that of these galaxies. The luminosity distribution of the quasars does not depend strongly on the visual threshold applied.

It is interesting to see if the luminosity distributions depend on the radio properties of the quasars, and in Figure 2 the quasar sample has been accordingly further subdivided. Here, and in the rest of this paper, the quasars are arbitrarily termed "radio quiet" if their luminosity at 6 cm as derived from the flux density given by VCV is less than $10^7\ L_\odot$ ($L_\nu < \sim 10^{24}$ W Hz^{-1}). It should be parenthetically noted that the radio quiet quasars could equally well have been defined as those with positive slopes between the 6 cm flux density and that measured at 60 μm. "Flat" spectrum radio sources are defined to be those quasars with a radio spectral index $\alpha_r > -0.4$ and the "steep" spectrum radio quasars are those with $\alpha_r < -0.7$. The radio spectral index α_r was calculated using the 6 cm flux densities given by VCV and, when available, the 74 cm flux densities from the literature (e.g., Dixon *et al.* 1970 and updates). Otherwise the 6 and 11 cm flux densities given by VCV were used. Of the 91 quasars in the sample with 6 cm flux density

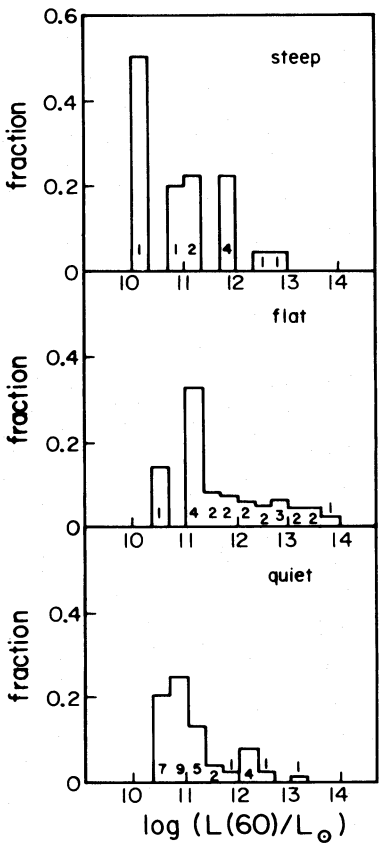

FIG. 2.—The fractional luminosity distributions at 60 μm of the entire sample of quasars separated according to their radio properties. The quasars are arbitrarily termed "radio quiet" if their luminosity at 6 cm as derived from the flux density given by VCV is $< 10^7\ L_\odot$. "Flat" spectrum radio sources are taken to be those quasars with a radio spectral index $\alpha_r > -0.4$ and the "steep" spectrum quasars are those with $\alpha_r < -0.7$. The radio data are from VCV and Dixon *et al.* (1970). The numbers correspond to the number of detections in each bin and indicate the low accuracy of the histograms.

© American Astronomical Society • Provided by the NASA Astrophysics Data System

1986ApJ...308..815N

greater than 300 mJy, 16 had spectral indexes intermediate between -0.4 and -0.7; four of these were detected in at least one *IRAS* band.

All of the quasars studied which have a redshift larger than $z = 1.00$, which were detected at one or more *IRAS* wavelengths, and which show radio emission above 300 mJy at 6 cm are flat radio spectrum sources. One steep radio spectrum quasar and one radio quiet quasar with $z > 1.00$ were also detected in at least one *IRAS* band; these—0597+561 and 1634+706—are discussed below. It is clear from Figure 2 that the radio quiet quasars, with a median infrared luminosity of 10^{11} $L_\odot$, are grouped toward lower luminosities, while the flat spectrum radio sources, with a median luminosity of $10^{12.3}$ $L_\odot$, extend toward significantly higher luminosities.

The distribution of the ratio of the luminosity at 60 μm to that in the visible, or alternatively of the 60 μm to visible spectral indexes, is displayed in Figure 3. It is seen that the ratio of luminosities varies by as much as a factor of 100 reflecting a range in the infrared to visual spectral index of 1.0. Several of the most extreme ratios are, however, undoubtedly artifacts of variability in the sources. As a specific example, 2223−052 (3C 446), with almost 100 times the luminosity in the infrared as in the visible, was undergoing an outburst in the infrared at the time the pointed observations were made, whereas the visual measurements (from VCV) were undoubtedly made when the quasar was more quiescent; see below. This variability is the cause of the most extreme luminosity ratio displayed by the flat radio spectrum sources and makes it uncertain what the intrinsic spread of the flat spectrum is. The cautions indicated by this example must be exercised whenever the *IRAS* observations are compared to observations made at different times, and particularly when discussing violently variable quasars.

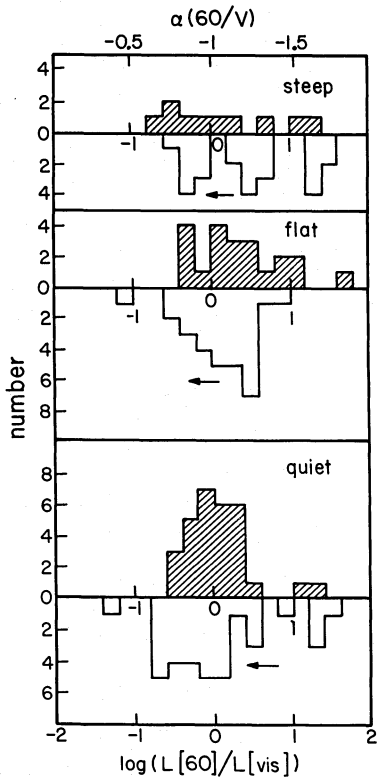

FIG. 3.—Histograms of log (L[60 μm]/L[vis]) for the quasars in the sample separated according to their radio properties as in Fig. 2. The approximate scale of spectral indexes between 60 μm and the visible (0.55 μm) is indicated at the top of the figure. The cross hatched upward-going histograms indicate detections with signal-to-noise ratios greater than 4. The downward-going open histograms indicate limits in the sense indicated by the arrows.

Figure 3 shows there is a clear correlation between the flux density at 60 μm and the flux densities measured in the visible for the radio quiet quasars. The validity of the broader distribution for quasars which vary is, as indicated above, uncertain, although formally the distributions indicate that the radio quiet and steep radio spectrum quasars have less infrared luminosity relative to the visible than do the flat radio spectrum quasars; i.e., the radio quiet and steep radio spectrum quasars exhibit slightly flatter slopes than do the flat radio spectrum quasars. The mean spectral index of the detected radio quiet and steep radio spectrum quasars between 60 μm and the visible is -1.04 ± 0.04, while that of the detected flat radio spectrum quasars is -1.19 ± 0.06 reflecting population dispersions of 0.24 and 0.26, respectively. The substantial number of upper limits indicates, however, that there may well be a population of quasars with very little infrared luminosity relative to that observed at the higher frequencies.

The *IRAS* measurements were also compared to the near-infrared (1.3 to 10.6 μm) observations available in the archives of the Caltech infrared group; most of these observations are published in Neugebauer *et al.* (1979) and Neugebauer *et al.* (1986). Nineteen radio quiet quasars with detections at 12 μm had also been measured at Palomar, generally within 3 yr of the *IRAS* measurements. The distribution of the 12 to 2.2 μm slopes of these 19 is essentially the same as that displayed in Figure 3 for the spectral index α(60/vis) of the radio quiet quasars in the sample. Thus there is no evidence for deviations from a smooth continuum in the near-infrared. There were not sufficient radio loud quasars with 12 μm detections and near-infrared measurements to compare the distribution of these slopes with those extending to the visible wavelengths, but the few measurements available showed no excursions outside those displayed in Figure 3.

b) Infrared Color-Color Plots

Plots of the infrared colors as measured by the spectral indexes in the *IRAS* bands are shown in Figures 4 and 5 for those quasars with detections in the relevant bands. Again the quasars are divided according to their radio properties. Similar color-color plots for Seyfert galaxies (Miley, Neugebauer, and Soifer 1985) and for bright galaxies having $f_\nu(60) > 5$ Jy selected from the *IRAS* survey by Soifer *et al.* (1986) are also included.

It is seen from Figures 4 and 5 that there is a considerable overlap between the quasars, the Seyfert galaxies, and the infrared bright galaxies. The bright galaxies, presumably being dominated by thermal emission, are more distinct from the Seyfert galaxies and the quasars than the latter two are from each other. Within a large amount of scatter, the Seyfert galaxies and the quasars are grouped around the line of constant spectral indexes. Although the Seyfert galaxies and quasars have approximately the same ranges in the three slopes presented, the quasars are more tightly grouped toward the flatter spectral indexes than are the Seyfert galaxies. There is no strong correlation between the radio properties and the location in the color-color plot.

The emission mechanisms responsible for the infrared radiation will be discussed below, but it is clear that the infrared

© American Astronomical Society • Provided by the NASA Astrophysics Data System

1986ApJ...308..815N

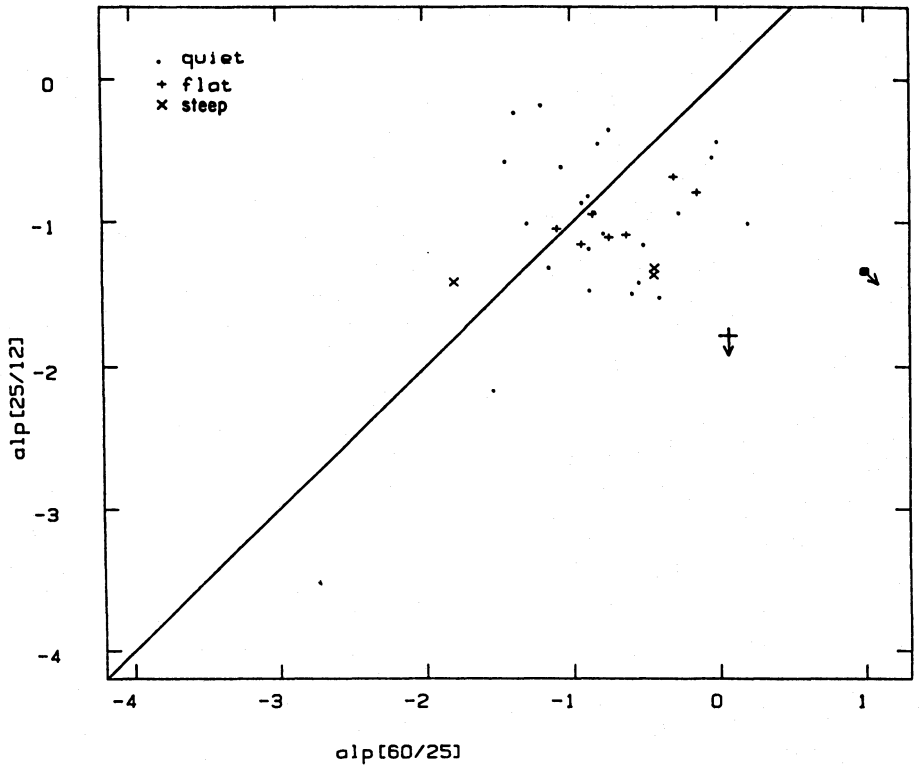

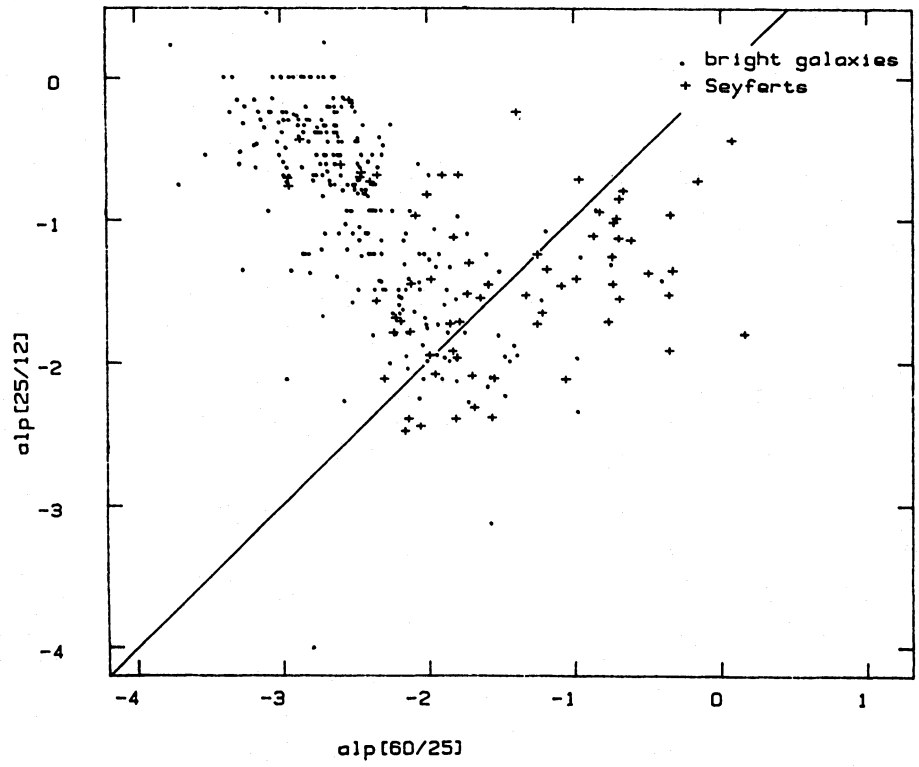

FIG. 4.—The spectral index between 25 and 12 μm, $\alpha(25/12)$, is plotted vs. the spectral index between 60 and 25 μm, $\alpha(60/25)$, for the quasars (*top panel*), and for the samples of Seyfert 1 and 2's and infrared bright galaxies as in Fig. 1. The solid line is drawn to indicate equal spectral indexes. In order to minimize confusion, only limits which require that quasars lie farther than one unit from this line are included. The quasars are divided according to their radio properties as in Fig. 1.

© American Astronomical Society • Provided by the NASA Astrophysics Data System

1986ApJ...308..815N

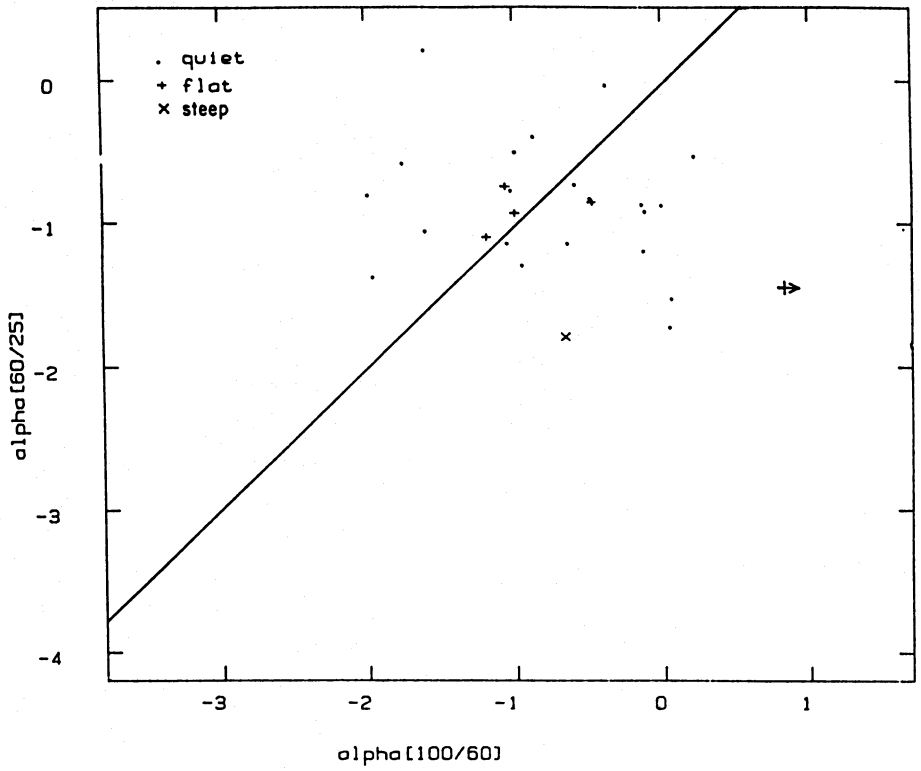

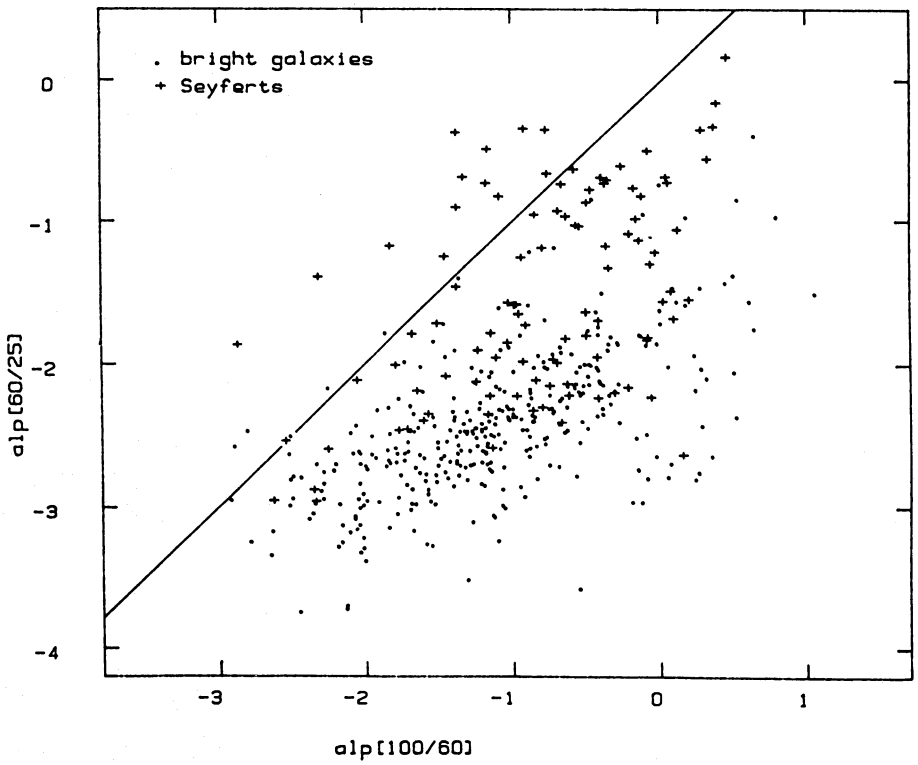

FIG. 5.—The same plots as shown in Fig. 4 are shown except that the spectral index $\alpha(60/25)$ is plotted against $\alpha(100/60)$, the spectral index between 100 and 60 μm. The three quasars with $\alpha(60/25) < -1.5$ correspond to 0134+329 (3C 48) [$\alpha(60/25) = -1.8$], 0157+001 (Mrk 1014) [$\alpha(60/25) = -1.75$], and 1254+571 (Mrk 231) [$\alpha(60/25) = -1.5$] while the highest index shown [$\alpha(60/25) = 0.2$], corresponds to (PG) 1211+143. The limit at $\alpha(100/60) = 0.8$ corresponds to the quasar (PKS) 2059+034.

© American Astronomical Society • Provided by the NASA Astrophysics Data System

1986ApJ...308..815N

colors, by themselves, do not distinguish whether the observed radiation is thermal or nonthermal. In Figure 5 three quasars by the luminosity definition of VCV—0134+329 (3C 48), 0157+001 (Mrk 1014), and 1254+571 (Mrk 231)—lie well below the line of constant spectral index and lie closer to the region occupied by Seyfert and most luminous infrared galaxies. Thus these quasars lie closer to the region of the color-color plot where thermal emission is potentially indicated. Mrk 1014 and Mrk 231 have also been classified as Seyfert galaxies. Cutri, Rieke, and Lebofsky (1984) have found evidence that Mrk 231 is either a giant elliptical galaxy or a less luminous galaxy undergoing a massive burst of star formation, while MacKenty and Stockton (1984) present evidence for a recent burst of star formation in Mrk 1014. Neugebauer, Soifer, and Miley (1985) have argued that the 60 μm emission in 3C 48 is thermal emission from a host galaxy associated with the quasar. Likewise, in Figure 5, the quasar 1211+143 lies well above and to the left of the line of equal spectral indexes, reflecting a bump at 25 μm which may be evidence for an added emission component. The indexes typical of the majority of the quasars can correspond to either thermal or nonthermal emission.

Neugebauer *et al.* (1984*b*) presented preliminary *IRAS* data on a small number of radio quiet and radio loud quasars and found an indication of excess 100 μm emission in two radio quiet quasars. The colors of the larger number of quasars presented in Figure 5, however, do not show evidence for such an excess and a resultant possible systematic difference between radio loud and radio quiet quasars.

The strength of the infrared emission relative to that in the visible and radio is illustrated in Figure 6 which shows the spectral indexes from 60 μm to the visible versus those from 6 cm to 60 μm for the radio loud quasars detected. It is seen that the spectral index from the radio to the infrared is typically flatter than that from the infrared to the visible and, especially for the steep spectrum radio sources, occupies a very narrow range of radio-to-infrared spectral indexes. The steep radio spectrum sources are also flatter in their radio-to-infrared indexes than are the flat radio spectrum sources. The color changes noted in Figures 4 and 5 are thus consistent features of an overall smooth energy distribution which has a transition from the flatter radio spectrum to a steeper spectral index at the higher frequencies.

If the emission is synchrotron radiation, the frequency at which this transition occurs is presumably related to the magnetic fields and geometry of the central source, and Jones *et al.* (1981) find the transition frequency remarkably constant in a sample of compact nonthermal sources. The transition frequency between a radio continuum assumed to have zero slope at the 6 cm flux density and the steeper 60 to 12 μm infrared slope was calculated for the radio loud quasars observed by *IRAS* as a function of the redshift of the quasar, but no strong correlation between the two was evident. Thus, to the extent that this definition of the transition frequency is valid, the

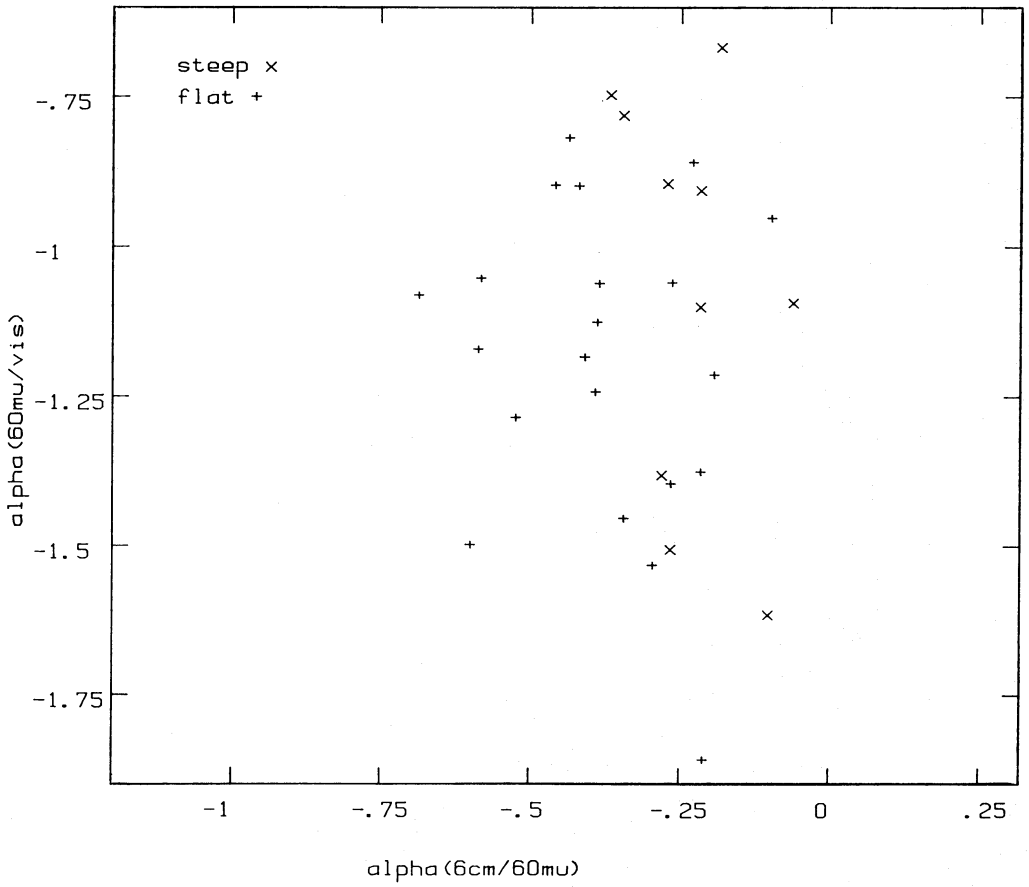

FIG. 6.—The infrared to visible spectral index, α(60 μm/vis), vs. the spectral index between the radio and infrared, α(6 cm/60 μm), is presented for radio loud quasars. Steep radio spectrum quasars are distinguished from flat radio spectrum sources. The visible magnitudes have been taken from VCV.

© American Astronomical Society • Provided by the NASA Astrophysics Data System

1986ApJ...308..815N

conditions which establish the transition frequency are not, within substantial spread, constant in the sample. The non-simultaneous nature of the radio and infrared observations and the lack of higher frequency radio observations weaken this conclusion. Other algorithms for finding the transition frequency resulted in no better correlations.

Miley, Neugebauer, and Soifer (1985) have shown there is a possible correlation between the 100 to 60 μm spectral index, $\alpha(100/60)$, of Seyfert galaxies and their luminosity near 60 μm. A similar correlation is shown by the galaxies in the sample of infrared bright galaxies (Soifer *et al.* 1986), presumably indicating that the correlation is related to the thermal or star-burst emission in the galaxies. Figure 7 extends this comparison to include the quasars and shows that in general the quasars exhibit no correlation between the slopes and the luminosity. Thus, the physical mechanisms or geometry effects responsible for the correlation in the Seyfert galaxies and the strong infrared galaxies do not dominate the infrared continuum in the quasars.

c) *Infrared Curvatures*

The trend in the slopes noted above implies there is a general curvature in the continuum between 100 and 12 μm. Increased curvature above the general curvature can be a signature of additional emission components in the quasars. As an example, Miley *et al.* (1984), in studying the active galaxy 3C 390.3, have interpreted increased curvature between 60 and 12 μm as indicating thermal emission at 25 μm.

The distributions of the 60 μm curvature, taken to be the difference $\alpha(100/60) - \alpha(60/25)$, and the 25 μm curvature, taken as the difference $\alpha(60/25) - \alpha(25/12)$, is shown in Figure 8. It is seen that the distributions of curvatures are quite uniform, and thus by themselves do not provide unique insight in determining whether or not an additional component above the smooth continuum is present. In particular, the active galaxy 3C 390.3 has a 25 μm curvature of 1.7 and the quasar 3C 48 has a 60 μm curvature of 1.1, putting them at one end of, but not extreme for, the distributions of infrared curvatures in Figure 8. As a comparison, the median 25 and 60 μm curvatures of the *IRAS* bright galaxies studied by Soifer *et al.* (1986) are -1.5 and 1.25.

Figure 9 shows that there is no strong correlation between the curvature measured in the energy distributions of the quasars and the luminosity at 60 and 25 μm as might be expected if significant far-infrared luminosity were associated with emission bumps at these wavelengths. There is, as to be expected, a correlation between the curvature and the spectral slopes in the sense that the highest curvatures in the quasars are associated with the steeper slopes. It should be noted that the quasar 0530−3755, which was detected primarily at

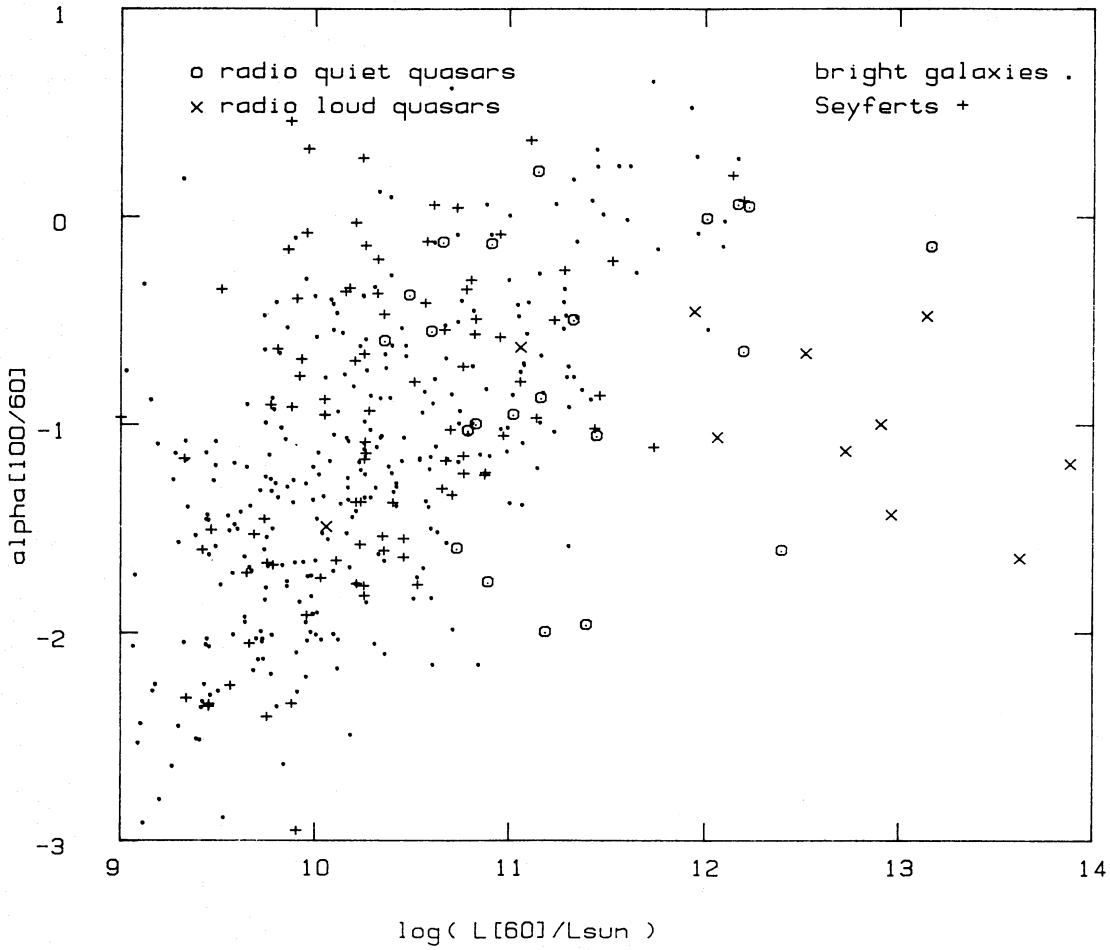

FIG. 7.—The spectral index $\alpha(100/60)$ is plotted vs. the luminosity at 60 μm for the quasars in this sample, for the infrared bright galaxy sample of Soifer *et al.* (1986), and for the Seyfert galaxies (Miley, Neugebauer, and Soifer 1985).

© American Astronomical Society • Provided by the NASA Astrophysics Data System

1986ApJ...308..815N

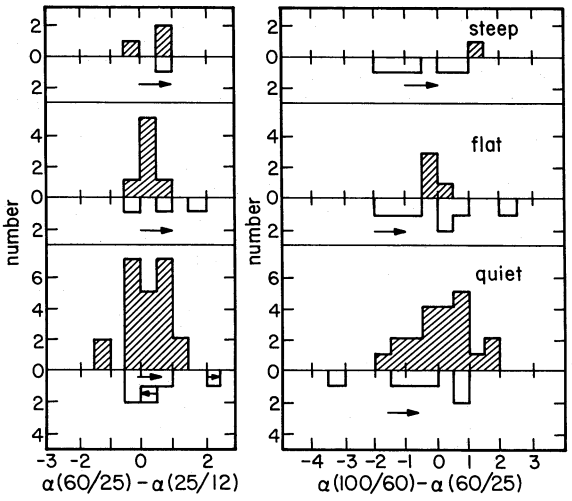

FIG. 8.—Histograms are presented of the curvature at 25 μm [α(60/25) − α(25/12)] and that at 60 μm [α(100/60) − α(60/25)]. The same convention as used in Fig. 3 is used. The quasars are divided according to their radio properties as in Fig. 2.

25 μm and thus might be a good candidate object in which to search for thermal emission, has a 25 cm curvature exceeding 0.1, not a conspicuous value.

d) Comparison with X-Ray Properties

Thirty-two of the quasars observed by *IRAS* have also been observed, primarily with the *Einstein Satellite*, at X-ray frequencies (Tananbaum *et al.* 1979; Zamorani *et al.* 1981; Owen, Helfand, and Spangler 1981; Tananbaum *et al.* 1983). The distributions of the spectral indexes, α(60/X), between the 60 μm and the X-ray measurements, and of the spectral indexes, α(12/X), between 12 μm and the X-ray region are shown in Figure 10. It is seen that the indexes are spread rather uniformly over a range of ∼0.5 for both cases. This range is approximately twice the width of the distribution of α(mm/X) found by Owen, Helfand, and Spangler (1981) for a sample of quasars which were strong at millimeter wavelengths. The extra width could be an artifact of variability or it could be evidence for thermal emission bumps in the infrared. Again, the infrared to X-ray spectral indexes of the quasars do not seem to be tightly correlated with their radio properties. The results are apparently in disagreement with the findings of Malkan (1984) who observed that the near-infrared to X-ray spectral indexes have a spread only of ∼0.2. Although the possibility that variability has increased the dispersion strongly cannot be ruled out, the relative frequency difference between the far- and near-infrared compared to that to the X-ray region make this possibility unlikely.

V. SELECTED OBJECTS

0838 + 70.—This radio quiet quasar is a strong infrared source in all the *IRAS* bands. At 12 and 25 μm, the infrared source is located within 3″ of the optical position of the quasar. At 60 μm the infrared source is offset from the optical position by 26″, mainly in the direction perpendicular to the scan direction, while at 100 μm it is offset by 70″ in the same direction.

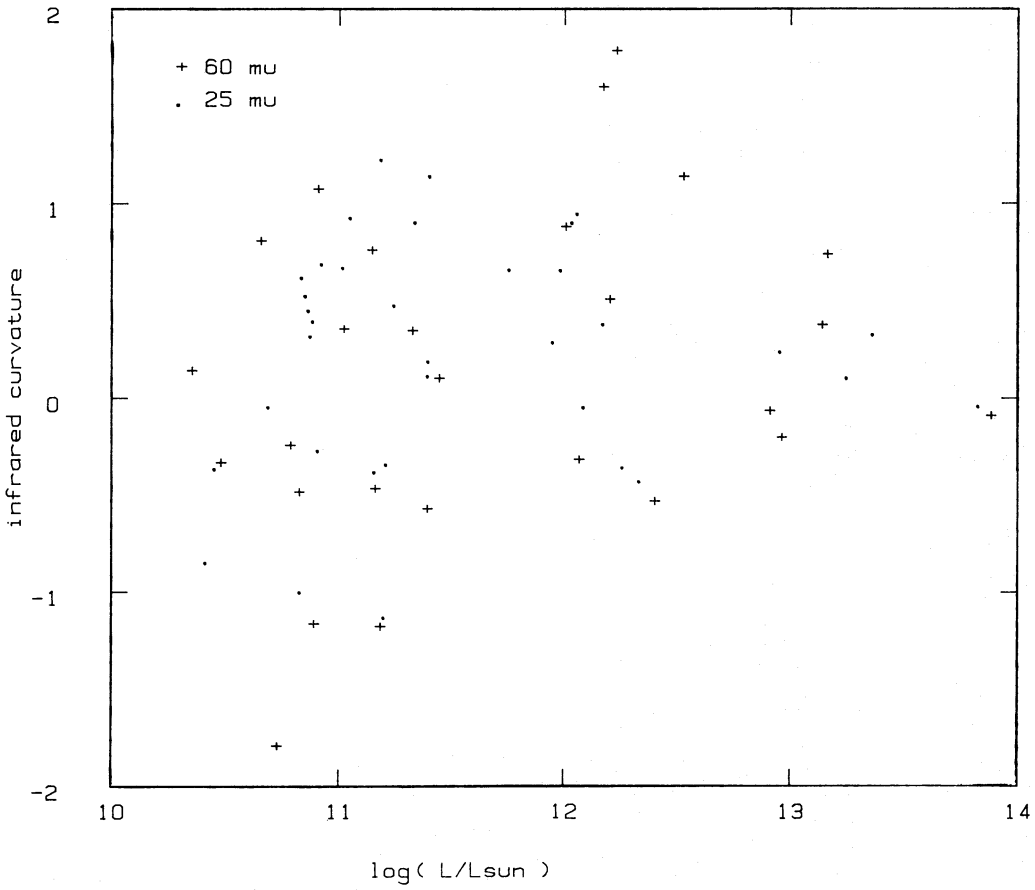

FIG. 9.—The infrared curvature at 25 μm, as defined for Fig. 8, is plotted vs. the luminosity at 25 μm and the curvature at 60 μm is plotted vs. the luminosity at 60 μm.

© American Astronomical Society • Provided by the NASA Astrophysics Data System

1986ApJ...308..815N

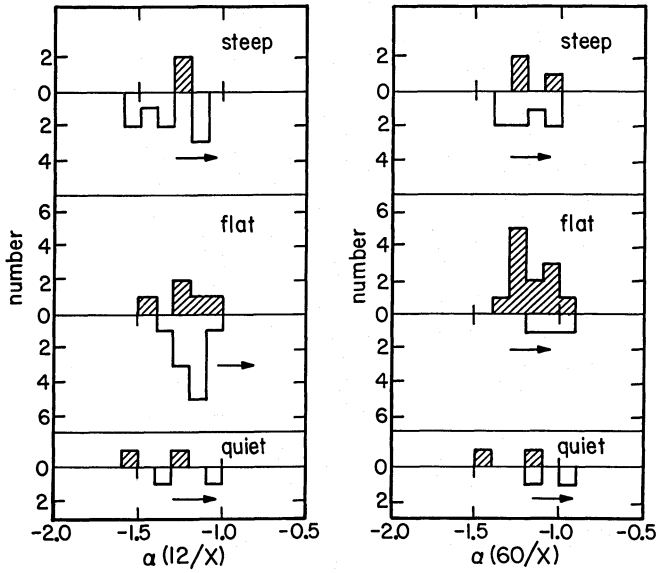

FIG. 10.—Histograms are given of the spectral indexes between 12 μm and the X-ray region, α(12/X), and of those between 60 μm and the X-ray region, α(60/X). The conventions of Fig. 3 are again used, and the quasars are divided according to their radio properties as in Fig. 2. The X-ray observations have been obtained from Tananbaum *et al.* (1979), Zamorani *et al.* (1981), Owen, Helfand, and Spangler (1981), and Tananbaum *et al.* (1983).

There are few sources in the area covered by the observation which are seen both at 25 and 100 μm, so it is hard to verify positional alignment, but the apparent coincidence of two other sources indicate that the offset is not an instrumental one. As seen in Figure 11, the field has some infrared cirrus, but the object is nonetheless relatively isolated. One possibility that cannot be ruled out, however, is that underlying cirrus distorts the position of the filtered source. Although it is impossible to remeasure this offset until the next generation of infrared satellite is flown, it is tempting to speculate that we are seeing evidence for a displaced galaxy associated with the quasar. There is no galaxy visible on the prints of the POSS. Since the angular separation observed corresponds to a linear separation of about 150 kpc, such a suggestion is clearly very speculative.

0957+561A, B.—The pair of quasars 0957+561A, B have been identified by Walsh, Carswell, and Weymann (1979) as images of a single quasar seen doubled through the lensing action of an intermediate galaxy. Young *et al.* (1980) estimated the galaxy had a redshift of 0.39 and a visual flux density of 0.12 mJy. The source was detected by *IRAS* only at 60 μm, and it is uncertain whether the detection—100 mJy—corresponds to the quasar or to the intermediate galaxy. The limits placed on the slopes of 0957+561 [$\alpha(100/60) > -2.1$; $\alpha(60/25) < -0.9$] are completely consistent, in Figure 5, with the colors of either quasars or of galaxies, and its luminosity—$6.7 \times 10^{12}\ L_\odot$—although high, is not unusually so for a quasar. If the detection corresponds to emission from the galaxy, the luminosity of the galaxy would be $5 \times 10^{11}\ L_\odot$, again high, but not uncommon for galaxies found in the *IRAS* survey (see, e.g., Soifer *et al.* 1986). Likewise, the mean ratio of the flux density at 60 μm to that in the visible for the galaxies studied by Soifer *et al.* ranges from 100 to 1000, encompassing the value of 800 obtained if the infrared originates in the galaxy. Thus it is impossible to definitely ascribe the detection to either the quasar or the lensing galaxy. The fact, however, that 0958+561 is one of two quasars with $z > 1$ which are not flat spectrum radio sources tends to strengthen the speculation that thermal emission from the galaxy is being observed.

1254+571 (Mrk 231).—This is the brightest quasar observed at 60 μm. As can be seen in Table 1, its infrared brightness exceeds by a factor of 10 that of any other quasar observed. The ratio of its infrared to visible flux densities is also significantly larger than the mean ratio for the other quasars. This is accompanied by almost the steepest spectral index of

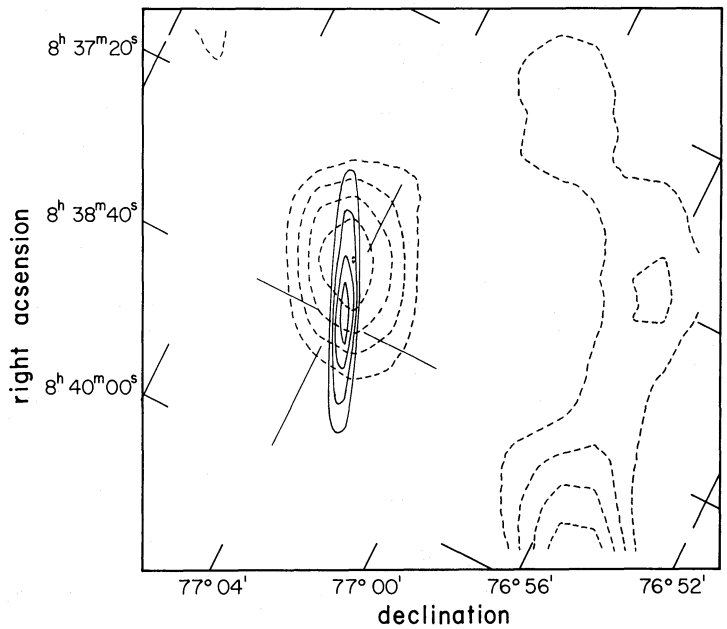

FIG. 11.—The spatially filtered contour plots of 0838+770 at 25 μm (*solid lines*) and at 100 μm (*dashed lines*) are shown. The displacement between the two centers and the presence of "cirrus" on the right hand side at 100 μm is apparent. The lowest contour lines represent twice the median noise level and the separation between contours is also twice the median noise. The horizontal axis is parallel to the direction of the scan motion of the telescope.

© American Astronomical Society • Provided by the NASA Astrophysics Data System

1986ApJ...308..815N

TABLE 2

NEAR- AND FAR-INFRARED MEASUREMENTS OF 2223−052 = 3C 446[a]

DATE	WAVELENGTH IN μm							
	1.3	1.65	2.2	10.6	12	25	60	100
1982 Sep 30	8.32	12.4	18.3					
1983 May 23	4.97	7.31	11.6					
1983 May 29–1983 Jun 8					<200	286	463	706
1983 Jul 22	5.15	7.80	12.2					
1983 Aug 20	14.2	20.7	32.4	202				
1983 Nov 11					168	363	951	1747
1984 Jun 8	1.85	3.02	5.08					
1984 Oct 8	1.29	2.05	2.98					

[a] Flux densities in mJy.
[b] On 1983 Aug 20, $f_\nu(3.7) = 60.3$ mJy.

any measured between 12 and 25 μm and the flattest index between 60 and 100 μm.

1634+706.—This radio quiet quasar is the only source in the present sample clearly identified with a quasar with a redshift $z > 1.0$ which is detected strongly. It exhibits high luminosity in all the *IRAS* bands. It is also extremely luminous in the visible with $M_B = -30.08$ mag (Schmidt and Green 1982). If the infrared emission is associated with thermal emission from heated dust, the grain temperature of the dust, based on the 60 to 100 μm colors, is approximately 96 K, thus requiring a mass of dust of only $\sim 2 \times 10^6\ M_\odot$.

2223−052 (3C 446).—The quasar 3C 446 is known to vary rapidly in the visible, the near-infrared, and at radio wavelengths. Table 2 and Figure 12 show the *IRAS* measurements along with near-infrared observations from Palomar Observatory. It is seen that in the near-infrared, 3C 446 underwent a burst in late 1983 which was reflected in almost constant near-infrared colors. Thus, unless it became precipitously fainter after 1983 August, it was always relatively bright in the near-infrared during the time of the *IRAS* observations. The *IRAS* measurements are consistent with an outburst occurring in the far-infrared also, although it is not clear whether the measured points are on the ascending or descending portion of the light curve. A comparison of the Palomar measurement at 10.6 μm in August with that made in November by *IRAS* at 12 μm would suggest that it was decreasing at the time of the *IRAS* measurements.

The rapid variability confirms that the dominant emission is nonthermal, as expected; the time scale sets the size of the far-infrared emitting region as less than half a light year. Although the *IRAS* measurements are too few and not sufficiently in time coincidence with those at other wavelengths, it is plausible, though unproved, that the far-infrared peak was, in fact, comparable in duration to that observed in the near-infrared; the size would then be restricted to the order of 0.1 pc. It is interesting to note that when 3C 446 was measured in November, its measured 60 μm luminosity, if isotropic, was $L(60\ \mu m) = 7.6 \times 10^{13}\ L_\odot$, the largest luminosity of any quasar measured by *IRAS* at 60 μm.

When the quasar was brighter, the far-infrared slopes were significantly steeper [$\alpha(100/60) = -1.2$, $\alpha(60/25) = -1.1$, $\alpha(25/12) = -1.05$] than when the quasar was fainter [$\alpha(100/60) = -0.8$, $\alpha(60/25) = -0.55$, $\alpha(25/12) < -0.5$]. The infrared curvatures in both cases were low, i.e., the points in the color-color plots of Figures 4 and 5 remained close to, or approached, the line of constant spectral index, completely consistent with nonthermal emission. Probably the most interesting aspect of the outburst is the small change at 25 μm relative to that at either the near-infrared wavelengths or at 60 and 100 μm. A plausible explanation for this is that, despite its location in the color-color plots, there is a nonvariable, presumably thermal, component present at 25 μm whose role is increased when the nonthermal component is low.

VI. COMPACT STEEP SPECTRUM RADIO QUASARS

The quasar 0134+329 (3C 48) is one of a population of compact, steep spectrum radio sources (Wilkinson *et al.* 1984; van Breugel, Miley, and Heckman 1984), and it is interesting to see if others in that class share the infrared properties of 3C 48. Of the quasars which these authors include in this class, four—3C 48, 1442+101, 1634+628 (3C 343), and 1828+487 (3C 380)—are in the sample studied here, and only 3C 48, with a luminosity corresponding to $\log (L[60]/L_\odot) \sim 12.5$ was detected at 60 μm. The luminosity limits at 60 μm of the latter three quasars are $\log (L[60]/L_\odot) < 13.6$, < 12.3, and < 11.8.

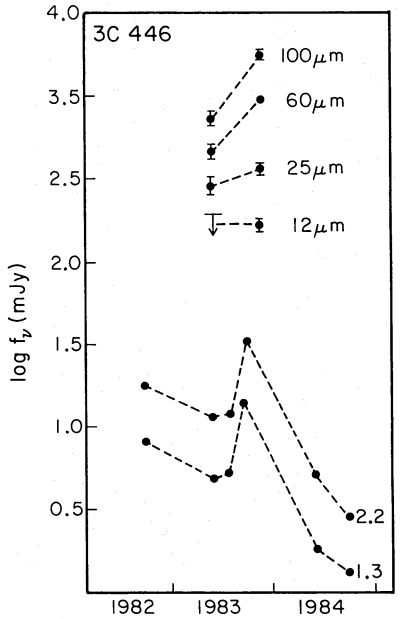

FIG. 12.—Near-infrared measurements at 1.3 and 2.2 μm and *IRAS* measurements of 3C 446 are presented vs. time. The dashed lines are merely to guide the eye between observations at the same wavelength and are not meant to represent the actual light curve. The near-infrared observations were obtained at Palomar Observatory.

© American Astronomical Society • Provided by the NASA Astrophysics Data System

1986ApJ...308..815N

The *IRAS* survey data of the other quasars in this class give no indication of a luminosity source in any of the quasars with a luminosity comparable to that of 3C 48, although most of the limits are poor. Thus the case of 3C 48 remains unique.

VII. EMISSION MECHANISM

There is strong circumstantial evidence from the observations that the infrared emission from the quasars whose radio emission has a flat spectrum is predominantly nonthermal in origin. For these objects the spectrum extends continuously through the infrared from a presumably nonthermal (often variable) radio nucleus to the presumably nonthermal (often variable) optical nucleus. Moreover, in the case of two of these flat-spectrum quasars, significant variability has actually been measured in the infrared.

For the quasars with steep radio spectra and the radio quiet quasars, the situation is less clear. The following points argue that the infrared emission from these objects is at least partially thermal in origin.

i) The luminosities for both steep radio spectrum and radio quiet quasars are systematically lower than those of the flat radio spectrum quasars, and, in contrast to the flat radio spectrum sources, they are not detected at high redshifts.

ii) For many quasars with steep radio spectra, and certainly for the radio quiet quasars, the infrared luminosity is considerably greater than their radio luminosity.

iii) For 3C 48, a steep radio spectrum quasar, Neugebauer, Soifer, and Miley (1985) conclude from a detailed study of the continuum energy distribution that the far-infrared emission is mainly thermal in origin.

iv) The N type radio galaxy 3C 390.3, if it were more distant, would be classified as a quasar with a steep spectrum radio source. This object has an infrared spectrum peaked close to 30 μm, and, although it was intensively monitored during the *IRAS* mission, no significant variability was detected. By analogy with NGC 1068 it has been concluded that the 3C 390.3 emission is thermal (Miley *et al.* 1984).

Although the arguments are not compelling, they lead us to lean toward a thermal interpretation for a portion of the infrared emission in quasars which are not associated with flat spectrum radio sources. This is presumed to arise from reradiation from dust in the narrow line regions (Miley and de Grijp 1985) and/or from a larger dust rich galaxy (Neugebauer, Soifer, and Miley 1985). A similar thermal component, if present in the flat spectrum objects, would frequently be swamped by the nonthermal emission.

To explore the consequences of a thermal model for the far-infrared emission in the radio quiet and steep spectrum quasars, the mass of dust required to produce the observed 60 μm and 100 μm flux densities for these quasars and the distance from the central luminosity source of the emitting material was estimated under the assumption that the heating of the dust is from the central quasar luminosity source and the dust is optically thin. The emissivity of the dust was taken to be $\epsilon \sim \nu^{1.5}$ and the mass absorption coefficient at 60 μm set equal to $\kappa_\nu(60\ \mu\text{m}) = 25\ \text{m}^2\ \text{kg}^{-1}$. The masses of dust ranged from $\sim 3 \times 10^5\ M_\odot$ to $\sim 5 \times 10^7\ M_\odot$. If the gas to dust ratio is ~ 200, the required total gas mass associated with this dust is 6×10^7 to $10^{10}\ M_\odot$. The distances at which the dust must reside from the central source are in the range 0.5–10 Kpc. These estimates are larger than the gas content believed associated with the narrow-line regions of normal quasars, but are quite consistent with the amount of gas that might be found in the host galaxy of the quasar. While not a proof of the thermal emission models, these numbers show that the models are consistent with the observations.

VIII. SUMMARY

The infrared flux densities of the flat radio spectrum quasars as measured by *IRAS* generally form a smooth interpolation between measurements in the visible and at radio wavelengths and offer few surprises. The luminosities near 60 μm of the flat spectrum radio sources extend to significantly higher values than do those of the radio quiet quasars or those with steep radio spectral indexes. The infrared luminosities range up to $10^{13.9}\ L_\odot$ and are generally comparable to those in the visible region. In some quasars, however, the infrared luminosities exceed the visible luminosities by an order of magnitude.

The infrared measurements are disappointing in that they provide no characteristic features which, by themselves, correlate strongly with the radio characteristics of the quasars or serve to define the mechanisms responsible for the large infrared luminosity of quasars. There are often suggestions of possible thermal emission peaks, but no cases where the statistics point overwhelmingly to thermal emission. Simultaneous measurements of the quasars extending over a wide range in frequency and especially in the submillimeter wavelengths are needed to provide a better picture of the nature of quasars and the role of the infrared emission. Far-infrared observations with high spatial resolution are also necessary to isolate the quasars from the host galaxies.

IRAS was successful because of the cooperative efforts of program managers, technical and engineering supporting staff, many scientific colleagues and the three supporting agencies, NASA, SERC, and NIVR. We thank Michael Rowan-Robinson, Gael Squibb, and Stella Harris, as well as the entire *IRAS* staff at Rutherford Laboratory, for their support in obtaining the pointed observations. We also thank Gene Kopan, Erick Young, Walter Rice, George Helou, and Linda Fullmer; they and the entire IPAC staff gave invaluable assistance with the reduction of the observations. Finally we thank Keith Matthews and Jay Elias for monitoring 3C 446 at the 200 inch (5.1 m) telescope at Palomar and C. Beichman for commenting extensively on the text. G. N. and B. T. S. were supported by the *IRAS* extended mission program; the ground-based observations at Palomar are supported by a grant from the National Science Foundation.

REFERENCES

Bregman, J. N., *et al.* 1986, in press.
Clegg, P. E., *et al.* 1983, *Ap. J.*, **273**, 58.
Cutri, R. M., Rieke, G. H., and Lebofsky, M. J. 1984, *Ap. J.*, **287**, 566.
Cutri, R. M., Wisniewski, W. Z., Rieke, G. H., and Lebofsky, M. J. 1985, *Ap. J.*, **296**, 423.
Dixon, R. S. 1970, *Ap. J. Suppl.*, **20**, 1.
Elvis, M., Maccacaro, T., Wilson, A. S., Ward, M. J., Penston, M. V., Fosbury, R. A. E., and Perola, G. C. 1978, *M.N.R.A.S.*, **183**, 129.
Glass, I. S. 1979, *M.N.R.A.S.*, **186**, 29P.
Harvey, P. M., Wilking, B. A., and Joy, M. 1982, *Ap. J. (Letters)*, **254**, L29.
IRAS Catalogs and Atlases, Explantory Supplement. 1985, ed. C. A. Beichman, G. Neugebauer, H. J. Habing, P. E. Clegg, and T. J. Chester (Washington, DC: US Government Printing Office).
IRAS Point Source Catalog. 1985, Joint *IRAS* Science Working Group (Washington, DC: US Government Printing Office).
Jones, T. W., Rudnick, L., Owen, F. N., Puschell, J. J., Ennis, D. J., and Werner, M. W. 1981, *Ap. J.*, **243**, 97.
Landau, R., *et al.* 1986, *Ap. J.*, **308**, in press.

© American Astronomical Society • Provided by the NASA Astrophysics Data System

1986ApJ...308..815N

Low, F. J., *et al.* 1984, *Ap. J.* (*Letters*), **278**, L19.
MacKenty, J. W., and Stockton, A. 1984, *Ap. J.*, **283**, 64.
Malkan, M. A. 1984, *Proc. Conference on X-ray and UV Emission from Active Galactic Nuclei*, ed. by W. Brinkmann and J. Trumper (Max Planck Institute for Physik und Astrophysik, MPE Report 184).
Meurs, E. J. A., and Wilson, A. S. 1984, *Astr. Ap.*, **136**, 206.
Miley, G. K., and de Grijp, R. 1985, Proceedings of First *IRAS* Symposium, Noordwijk, Preprint.
Miley, G., Neugebauer, G., Clegg, P. E., Harris, S., Rowan-Robinson, M., Soifer, B. T. and Young, E. 1984, *Ap. J.* (*Letters*), **278**, L79.
Miley, G. K., Neugebauer, G., and Soifer, B. T. 1985, *Ap. J.* (*Letters*), **293**, L11.
Neugebauer, G., *et al.* 1984*a*, *Ap. J.* (*Letters*), **278**, L1.
Neugebauer, G., Green, R., Matthews, K., Schmidt, M., Soifer, B. T., and Bennett, J. 1986, *Ap J. Suppl.*, submitted.
Neugebauer, G., Oke, J. B., Becklin, E. E., and Matthews, K. 1979, *Ap. J.*, **230**, 79.
Neugebauer, G., Soifer, B. T., and Miley, G. 1985, *Ap. J.* (*Letters*), **295**, L27.
Neugebauer, G., Soifer, B. T., Miley, G., Young, E., Beichman, C. A., Clegg, P. E., Habing, H. J., Harris, S., Low, F. J., and Rowan-Robinson, M. 1984*b*, *Ap. J.* (*Letters*), **278**, L83.
Owen, F. N., Helfand, D. J., and Spangler, S. R. 1981, *Ap. J.* (*Letters*), **250**, L55.
Schmidt, M., and Green, R. F. 1983, *Ap. J.*, **269**, 352.
Soifer, B. T., *et al.* 1986, in preparation.
Tananbaum, H., *et al.* 1979, *Ap. J.* (*Letters*), **234**, L9.
Tananbaum, H., Wardle, J. F. C., Zamorani, G., and Avni, Y., 1983, *Ap. J.*, **268**, 60.
Veron-Cetty, M. P., and Veron, P. 1985, *European Southern Observatory Scientific Report*, No. 4, 2d ed. (VCV).
van Breugel, W., Miley, G., and Heckman, T. 1984, *A.J.*, **89**, 5.
Walsh, D., Carswell, R. F., and Weymann, R. J. 1979, *Nature*, **279**, 381.
Wilkinson, P. N., Spencer, R. E., Readhead, A. C. S., Pearson, T. J., and Simon, R. S. 1984, in *IAU Symposium 110, VLBI and Compact Radio Sources*, ed. R. Fanti, K. Kellermann, and G. Setti (Dordrecht: Reidel), p. 25.
Young, E. T., Neugebauer, G., Kopan, E. L., Benson, R. D., Conrow, T. P., Rice, W. L., and Gregorich, D. T. 1985, IPAC Preprint No. PRE-008N.
Young, P., Gunn, J. E., Kristian, J., Oke, J. B., and Westphal, J. A. 1980, *Ap. J.*, **241**, 507.
Zamorani, G., *et al.* 1981, *Ap. J.*, **245**, 357.

P. E. CLEGG: Department of Physics, Queen Mary College, Mile End Road, London E1 4NS, England, UK

G. K. MILEY: Space Telescope Science Institute, Homewood Campus, The Johns Hopkins University, Baltimore, MD 21218

G. NEUGEBAUER and B. T. SOIFER: California Institute of Technology, George W. Downs Laboratory of Physics, 320-47, Pasadena, CA 91125

© American Astronomical Society • Provided by the NASA Astrophysics Data System